DOI: 10.1534/genetics.109.112532

Unified Framework to Evaluate Panmixia and Migration Direction Among Multiple Sampling Locations

Peter Beerli[1] **and Michal Palczewski**

Department of Scientific Computing, Florida State University, Tallahassee, Florida 32306

Manuscript received November 27, 2009
Accepted for publication February 17, 2010

ABSTRACT

For many biological investigations, groups of individuals are genetically sampled from several geographic locations. These sampling locations often do not reflect the genetic population structure. We describe a framework using marginal likelihoods to compare and order structured population models, such as testing whether the sampling locations belong to the same randomly mating population or comparing unidirectional and multidirectional gene flow models. In the context of inferences employing Markov chain Monte Carlo methods, the accuracy of the marginal likelihoods depends heavily on the approximation method used to calculate the marginal likelihood. Two methods, modified thermodynamic integration and a stabilized harmonic mean estimator, are compared. With finite Markov chain Monte Carlo run lengths, the harmonic mean estimator may not be consistent. Thermodynamic integration, in contrast, delivers considerably better estimates of the marginal likelihood. The choice of prior distributions does not influence the order and choice of the better models when the marginal likelihood is estimated using thermodynamic integration, whereas with the harmonic mean estimator the influence of the prior is pronounced and the order of the models changes. The approximation of marginal likelihood using thermodynamic integration in MIGRATE allows the evaluation of complex population genetic models, not only of whether sampling locations belong to a single panmictic population, but also of competing complex structured population models.

INVESTIGATIONS using genetic samples from individuals taken across a geographic or biological range—for example, water frogs caught at several ponds, blood samples of humans collected in several villages, or viruses collected from different host species that have the same disease—are common. Whether the individuals studied belong to a single population that is long-term randomly mating or to two or more populations that have varying degrees of genetic isolation from each other is an important concern. Because the geographic information about the locations often does not give a clear indication about the degree of genetic isolation of the individuals, we often use the genetic data themselves to calculate test statistics to suggest whether or not the locations belong to the same population. Many programs (Hudson *et al.* 1992b; Michalakis and Excoffier 1996; Rousset 1996; Neigel 2002; Weir and Hill 2002; Holsinger *et al.* 2002) use allele frequencies to calculate F_{ST} for pairs of locations or use Fisher's exact test to reject panmixia for the whole or subsets of the data (Raymond and Rousset 1995; Rousset 2008).

Several methods test explicitly whether two populations are or are not panmictic (for example, Hudson *et al.* 1992a; Rousset 1996). These methods are often applied to all pairs of a multiple-population data set. This is problematic, because both Beerli (2004) and Slatkin (2005) have shown that pairwise analyses can inflate the effective population size estimates, thereby confounding estimators of migration that use the effective number of migrants.

Alternatives to tests based on allele frequencies have been implemented, for example, in the programs STRUCTURE (Pritchard *et al.* 2000), BAPS (Corander *et al.* 2008), and STRUCTURAMA (Huelsenbeck and Andolfatto 2007). These methods allow the assignment of individuals to groups using the compatibility of their multilocus genotypes. They can thus be used to group locations into panmictic units on the basis of allele profiles and geography; this capability led to many advancements in landscape genetics and phylogeography. If we are interested in directionality of migration, however, this framework is often insufficient because the assignment methods offer only limited insight into population processes, such as migration, mutation, or fluctuation of population size, that underlie and account for the present genetic structure (Palsbøll *et al.* 2007).

We describe here another alternative, using Bayesian inference, that calculates probabilities of explicit population models using coalescence theory (a historical

Supporting information is available online at http://www.genetics.org/cgi/content/full/genetics.109.112532/DC1.

[1] *Corresponding author:* Department of Scientific Computing, Dirac Science Library 150-T, Mailbox 4120, Florida State University, Tallahassee, FL 32306-4120. E-mail: beerli@fsu.edu

review is given by Kingman 2000). An extension of the original n-coalescent of Kingman to multiple populations with migration (Strobeck 1987; Hudson 1991) leads to probabilistic inference programs that consider potentially complex migration patterns among sampling locations (for example, Beerli and Felsenstein 2001; Beerli 2006; Kuhner 2006). The program MIGRATE (Beerli and Felsenstein 2001; Beerli 2006) allows the calculation of a likelihood ratio test (LRT) for nested population models, but these calculations only approximate the LRT (Beerli 2008), need a moderately complicated approach with several independent runs (Beerli 2009), or require time-consuming large-scale simulations (Carstens *et al.* 2005). In our approach, a Bayes factor (BF) takes the role of an LRT. BFs and LRTs are not equivalent, however: the BF is the ratio of the marginal likelihoods of two hypotheses M_1 and M_2, whereas the LRT measures support for one hypothesis over another at the maximum likelihood. BFs are better suited for model selection than LRTs because one can compare nonnested as well as nested models. In addition, the programming and the successful application of Bayesian inference programs are often simpler than maximum likelihood (Beerli 2006).

Here, we report on the effect of two different approximations of the marginal likelihood on BF and therefore on the support for specific population models. We provide examples of the use of these methods to extend our tool set for investigating whether sampling locations are part of a panmictic population or are parts of a more complex population structure. Our approach unifies the analysis of population models and allows a wide spectrum of comparisons, from simple tests of whether locations sampled are part of a single population to more complex questions, such as whether there are unambiguous migration directions among populations; it also calculates posterior distributions of parameters of these models.

MATERIALS AND METHODS

Our approach to population model selection uses a framework that allows inferring parameters using coalescence theory. The population models are simple structured coalescence models with possibly many parameters (Beerli and Felsenstein 2001).

Bayes Factor estimation: In a typical Bayesian inference using Markov chain Monte Carlo (MCMC) methods we do not need to calculate the marginal likelihood to estimate the posterior probability distribution of the parameters of a specific model because the MCMC analysis depends only on likelihood ratios and not absolute likelihoods. Because BF is a ratio of marginal likelihoods of two models, however, calculation of these absolute likelihoods is essential. Because we use absolute likelihoods, we can now easily compare more than two models with the BF framework by choosing a reference model and comparing or ranking other candidate models with that.

We augmented the program MIGRATE (Beerli 2006) with a module to calculate the marginal likelihood

$$L_{M_i} = P(D \mid M_i) = \int_{\Psi_i} P(\Psi_i \mid M_i) P(D \mid \Psi_i, M_i) d\Psi_i, \qquad (1)$$

which is the probability density of the data where the parameters, for example population sizes and migration rates, and nuisance parameters, for example genealogies Ψ_i, of the model M_i are integrated out using the prior distribution $P(\Psi_i|M_i)$. The marginal likelihood is difficult to estimate with sufficient accuracy because not only the region around the mode, but also the tails of the distribution need to be explored. This is not straightforward in an MCMC context where we bias toward more likely solutions and so have a tendency to sample the tails of the distribution less frequently. The marginal likelihood is calculated in a Bayesian context and needs proper prior distributions to exist. Improper priors would lead to infinitely large tails that do not allow a consistent estimate of the marginal likelihood. We contrast two different methods to estimate the marginal likelihood: harmonic mean (Newton and Raftery 1994; Kass and Raftery 1995) and path sampling (Gelman and Meng 1998). Studies of path sampling have recently led to an alternative method of estimating marginal likelihoods (thermodynamic integration) (Gelman and Meng 1998; Lartillot and Philippe 2006; Friel and Pettitt 2005, 2008).

Harmonic mean estimator: Newton and Raftery (1994) described an approximation of Equation 1 using a harmonic mean estimator. Our stabilized harmonic mean estimator is a natural adaptation of Newton and Raftery's harmonic mean estimator to problems that treat genealogies as nuisance parameters and summarize over all possible genealogies G using the Metropolis–Hastings algorithm (our MCMC sampler was described in detail by Beerli 1998, 2006 and Beerli and Felsenstein 1999, 2001). We approximate the marginal likelihood as

$$L_{\mathrm{HM}} = P(D \mid M_i) \approx \left(\frac{1}{m} \sum_{j=1}^{m} \frac{1}{P(D \mid G_j)} \right)^{-1}. \qquad (2)$$

The extension from single-locus to multilocus data is not straightforward even with unlinked loci. We developed a method for combining independently inferred marginal likelihoods that allows fast parallel computation of unlinked loci. The combined marginal likelihoods are the product of the independent marginal likelihoods for each locus and a scaling factor K for loci,

$$L_{\mathrm{HM}}^{(\mathrm{all})} = K \prod_{z=1}^{Z} P(D_z \mid M_i). \qquad (3)$$

The scaling factor

$$K = \int_{\mathcal{P}} \prod_{z}^{Z} P(D_z \mid \mathcal{P}, M_i) P(\mathcal{P} \mid M_i)^{1-Z} d\mathcal{P}, \qquad (4)$$

where Z is the number of loci. We describe the scaling factor K in detail in the appendix. K can be approximated using prior, likelihood, and posterior values reported during the MCMC run (appendix). Our program MIGRATE version 3.1 calculates K and reports locus-specific and combined marginal-likelihood values when multiple loci are used.

Path sampling or thermodynamic integration estimator: MCMC sampling spends more time in areas of the search space proportional to the likelihood; as a result little attention is paid to regions with low likelihoods despite the fact that they may be large. Marginal likelihood is the integral over the whole search space and therefore may depend on accurate representation of these low-likelihood areas. Path sampling allows exploring these low-likelihood areas by distorting the acceptance ratio of the MCMC procedure with scaling factor τ ranging from zero to 1.0, where at $\tau = 0.0$ the process samples from the prior distribution and at $\tau = 1.0$ it samples from the distribution of interest. Thus, we calculate the log marginal likelihood using the expectation of the distribution of all coalescent genealogies G given the data D evaluated at scaling factor τ,

$$\ell_{\text{TI}} = \ln P(D \mid M_i) = \int_0^1 \mathbb{E}_{G \mid D,\tau} \ln P(D \mid G, M_i) d\tau. \qquad (5)$$

We approximate this integral using the trapezoidal rule for the scaling factor τ, using a small number of scaling values $\tau_0 = 0 < \tau_1 < \ldots < \tau_k < \ldots < \tau_n = 1$ and the corresponding marginal likelihoods $y_0 \ldots y_n$ as

$$\ell_{\text{TI}} = \sum_{k=2}^{n} (\tau_k - \tau_{k-1}) \frac{y_k + y_{k-1}}{2} \qquad (6)$$

with the average of log likelihoods, $\ln \text{P}(D \mid G_j, M_i)$, at a given scaling value τ_k,

$$y_z = \frac{1}{m} \sum_{j=1}^{m} \ln P_{\tau_k}(D \mid G_j, M_i). \qquad (7)$$

For multiple unlinked loci we then use

$$\ell_{\text{TI}}^{(\text{all})} = \ln K \sum_{z=1}^{Z} \ell_{\text{TI}}^{z}. \qquad (8)$$

The K is the same as the one in Equation 4. MIGRATE already used a scheme to run parallel MCMC chains to improve the exploration of search space using discrete scaling values τ_k that is based on the scheme proposed by Geyer and Thompson (1995): Metropolis coupled Markov chain Monte Carlo (MCMCMC). They formulated their method in terms of thermodynamic properties in which a chain that accepts always, with $\tau = 0.0$, is the hottest chain with a temperature of $1/\tau = \infty$ because the chain bounces randomly in many different areas of the search space, and a chain with $\tau = 1.0$ is cold because its movements are smaller. After each chain attempts a change of the genealogy, the system allows for swapping trees among neighboring MCMC chains with scaling factors τ_i and τ_{i+1} to improve the parameter estimates. The swap ratio depends on the relative likelihood ratios of randomly chosen pairs of chains with different τ and is

$$r < \frac{P(D \mid G_i)^{\tau_{i-1}} P(D \mid G_{i-1})^{\tau_i}}{P(D \mid G_i)^{\tau_i} P(D \mid G_{i-1})^{\tau_{i-1}}}, \quad 1 < i < n, \qquad (9)$$

where r is a uniform random number between 0 and 1, and n is the number of chains with different scaling factors τ. We use the term scaling classes to express the different discrete classes with different values of τ. One could express the same classes as temperature classes where the temperature T_i is $1/\tau_i$.

For the thermodynamic integration we record the likelihood values for each chain; these values are then used to calculate the averages y_k, which are used to calculate the marginal likelihoods. This is a static variant of the step-stone method proposed by Wangang Xie, Ming-Hiu Chen, Yu Fan, Lynn Kuo, and Paul Lewis (L. Kuo and P. Lewis, personal communication in 2008).

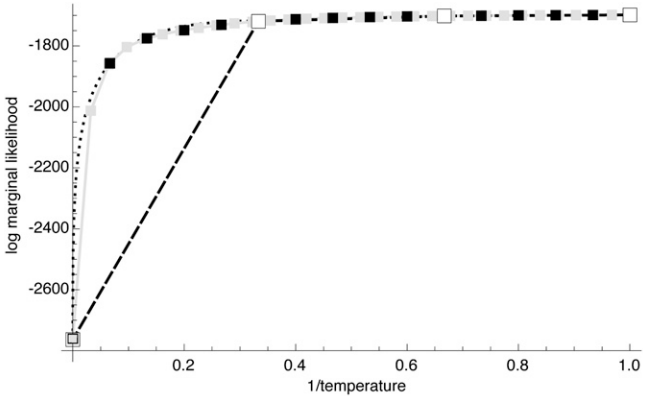

Figure 1.—Comparison of integration accuracy. The shaded curve with shaded squares shows means of 32 chains at equally spaced intervals of τ. Solid squares mark the curve derived from 16 chains. The dashed line marks the curve from 4 chains. The dotted line is the cubic Bézier-spline approximation of the first interval of the 4-chain run.

Using discrete classes τ_k may be too simple for phylogenetic applications (*cf.* Lartillot and Philippe 2006), but results in consistent estimates even for few scaling classes (Figure 1), except that the magnitudes of the estimates of the marginal likelihood (the area under the curve) are correlated with the number of scaling classes. The calculation time for each scaling class is about the same, so a run with 4 scaling classes will be about eight times faster than a run with 32 scaling classes. In principle, the different chains can be run in parallel, but the gain in speed is limited because the chains run in lockstep and need to wait on the slowest chain. Because many simulations (not shown) revealed that the shape of the path sampling function (Figure 1) is very similar with different migration models, we propose a different treatment of the first (the hottest) interval, defined by the scaling factors τ_0 and τ_1 with log-likelihood values y_0 and y_1, respectively. We calculate the area of this first interval analytically, using a cubic Bézier spline with two additional control points $c^{(0)}$ and $c^{(1)}$ that are calculated using the first three points. A point is a pair of τ_i and log-likelihood y_i and is defined as $p_i = (\tau_i, y_i)$. The additional control points are

$$c^{(0)} = \left(\tau_0, \frac{1}{5} y_0 + \frac{4}{5} y_1\right) \qquad (10)$$

$$c^{(1)} = \left(\tau_0, \frac{\tau_1 y_2 - \tau_2 y_1}{\tau_1 - \tau_2}\right) \qquad (11)$$

so that we have four control points

$$p_{\tau,y} = ((\tau_0, y_0), c^{(0)}, c^{(1)}, (\tau_1, y_1)). \qquad (12)$$

The values of the y-axis of the additional control points were chosen so that the Bézier curve mimics the path sampling function estimated with many scaling classes. We calculate a point $p^{(w)}$ on the Bézier function using

$$p_{\tau,y}^{(w)}(t) = \sum_{i=0}^{3} \binom{3}{i} p_{\tau,y}^{(i)} t^{i(1-t)^{3-1}}. \qquad (13)$$

The partial marginal likelihood by integrating the parametric function over the hottest interval is then

$$\ell_{(\tau_0,\tau_1)} = \int_0^1 p_y^{(w)}(\tau) \frac{dp_\tau^{(w)}}{d\tau} d\tau \qquad (14)$$

$$= \frac{1}{20}((\tau_1 - \tau_0)(y_0 + 3c_y^{(0)} + 6c_y^{(1)} + 10y_1)). \qquad (15)$$

This Bézier quadrature allows shorter run times than approaches with more scaling classes, an important fact because the estimation of large problems with many parameters can take a long time to run.

Simulation studies to test the approximations to the marginal likelihood: The quality of the two estimators $\hat{\ell}_{\mathrm{TI}}$ and $\hat{\ell}_{\mathrm{HM}}$ was tested using simulated data. These data sets were generated using a coalescence-based simulator (distributed from http://people.sc.fsu.edu/~beerli/programs).

One- and two-population simulations: The HM and TI approximations were compared with a standard test statistic based on allele frequencies (Hudson *et al.* 1992a), using two groups of simulated two-population data:

1. One hundred artificial DNA data sets containing 1000 sites for 10 individuals in each of two populations using a model with no immigration into population 2 with parameters $\Theta_1 = 0.005$, $\Theta_2 = 0.01$, $M_{2\to1} = 100$, $M_{1\to2} = 0$ were analyzed with nine different models. Θ is the mutation-scaled effective population size, $4N_e\mu$, and M is the ratio of the immigration rate m and the mutation rate μ per site and generation. The marginal likelihoods of eight alternative models were then compared with the marginal likelihood of the model used to simulate the data, the "true" model. This comparison of marginal likelihood ratios is equivalent to Bayes factors.
2. Simulations of four sets of 100 single-locus data sets with different degrees of isolation from each other were used to compare the Bayes factor method against a traditional test based on frequencies. These four sets were simulated with (a) $\Theta = 0.01$ and the 20 individuals randomly split into two groups; (b) $\Theta_1 = \Theta_2 = 0.005$, $M_{2\to1} = M_{1\to2} = 500{,}000$ (this is equivalent to a total $Nm = 1250$); (c) $\Theta_1 = \Theta_2 = 0.005$, $M_{2\to1} = M_{1\to2} = 100$ (this is equivalent to a total $Nm = 0.25$); and (d) $\Theta_1 = \Theta_2 = 0.005$, $M_{2\to1} = M_{1\to2} = 1$ (this is equivalent to a total $Nm = 0.0025$). The analyses of these four sets were done for two models, a single-population model and a full two-population model.

Large-scale population simulations: Many real problems include many sampling locations for which the association of sampling locations and panmictic populations is unknown. We simulated data for 50 loci from 3 populations using a scenario as outlined in Figure 2A. This stepping-stone model has five parameters and for each locus 300 bp were simulated using these values: $\Theta_1 = 0.003$, $\Theta_2 = 0.003$, $\Theta_3 = 0.004$, $M_{1\to2} = 100$, $M_{2\to3} = 100$. The individuals (120, 120, and 160) in the 3 populations were then randomly grouped into 6, 6, and 8 sampling locations, respectively. The full data set contained 20 locations with 20 individuals each. These particular settings were chosen because they mimic potential data sets that use anonymous loci from the nuclear genome. A naive application of these data would ask for a 20-population analysis. With a default MIGRATE run we would need to estimate 20 population sizes and 380 migration parameters, a daunting task with few loci. A total of six potential migration models using different numbers of populations and different migration models were explored. The six cases presented use models with 1, 2, 3, and 20 populations with several candidate models (Table 1, Figure 2). Specific MIGRATE run conditions are described in supporting information, File S1.

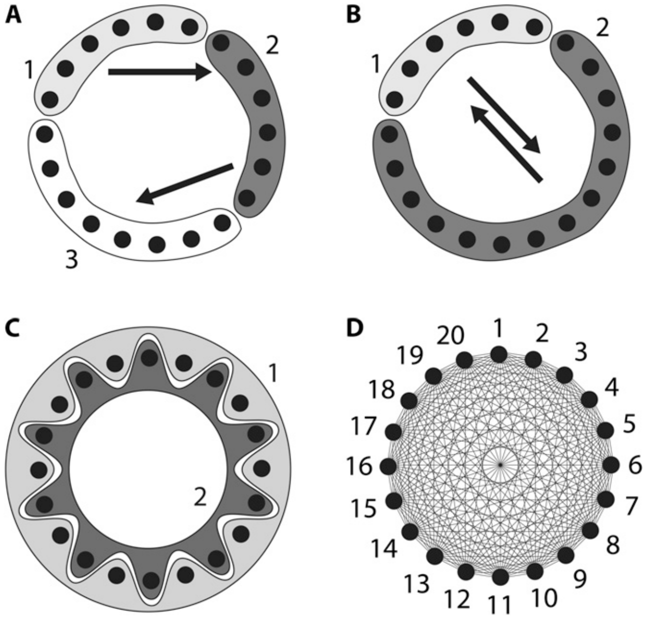

Figure 2.—Population structures used to generate artificial data sets. (A) The true population model, where population 3 receives immigrants from population 2, which receives immigrants from population 1. Each solid disk represents a random sample from the population and therefore represents an arbitrary sample subdivision (location sample) of the panmictic population 1, or 2, or 3. (A–C) show alternative partitionings used of the true population model. (B) The 20 location samples are lumped into 2 populations, combining populations 2 and 3 (see A). (C) An alternative 2-population model. (D) A naive 20-population model assuming each sampling location represents a population; arrows in A, B, and lines in D represent potential migration routes; migration routes in C are bidirectional from dark to light locations.

TABLE 1

List of migration models used for simulation study

No.	Pop.	Loc.	Param.	Description (numbers are location numbers)
1	3	20	5	$(1,2,3,4,5,6) \rightarrow (7,8,9,10,11,12) \rightarrow (13,14,15,16,17,18,19,20)$[a]
2	3	20	9	$(1,2,3,4,5,6) \rightleftharpoons (7,8,9,10,11,12) \rightleftharpoons (13,14,15,16,17,18,19,20) \rightleftharpoons (1,2,3,4,5,6)$
3	2	20	4	$(1,2,3,4,5,6) \rightleftharpoons (7,8,9,10,11,12,13,14,15,16,17,18,19,20)$[b]
4	2	20	4	$(1,3,5,7,9,11,13,15,17,19) \rightleftharpoons (2,4,6,8,10,12,14,16,18,20)$[c]
5	1	20	1	(1, 2, 3, 4, 5, 6, 7, 8, 9, 10, 11, 12, 13, 14, 15, 16, 17, 18, 19, 20)
6	20	20	400	(1) (2) (3) (4) (5) (6) (7) (8) (9) (10) (11) (12) (13) (14) (15) (16) (17) (18) (19) (20)[d]

No., model number; Pop., population; Loc., location; Param., parameter.

[a] See Figure 2A (true model).

[b] See Figure 2B.

[c] See Figure 2C.

[d] Each location is connected with all others; see Figure 2D.

Effect of prior choice and prior range: We explored the effect of the choice of the prior distribution on the marginal likelihood by using simulated multilocation single-locus data. We compared two exponential and two uniform prior distributions: narrow uniform prior distribution for Θ and M with a minimum of 0.00001, 0.0 and a maximum of 0.1, 5000, respectively; a wide uniform distribution with a maximum for Θ and M of 0.5 and 50,000; a narrow exponential distribution with the same minimum and maximum as the narrow uniform but a mean of 0.01 and 100 for Θ and M, respectively; and a wide exponential distribution with minimum and maximum of the wide uniform, but with a mean of 0.1 and 1000, respectively. Specific MIGRATE run conditions are described in File S1.

Model selection: Model choice probabilities s_i were calculated as suggested by Kass and Raftery (1995) by

$$s_i = \frac{\mathrm{BF}_i}{\sum_j^n \mathrm{BF}_j}. \qquad (16)$$

Example data set: Our example problem reanalyzes part of a data set of humpback whales from four sampling locations in the Southern Atlantic collected by Engel *et al.* (2008): near Brazil, Antarctica 1 (west of the Antarctic peninsula), Antarctica 2 (east of the Antarctic peninsula), and Colombia (Figure 1 in Engel *et al.* 2008). The data were analyzed using several different migration models. We used three subsamples of the original data, two with 10 and one with 30 randomly selected individuals from each location. We also ran one of the data sets twice for all example models to assess the effect of the Markov chain Monte Carlo error. We established a most likely mutation model within the constraints for MIGRATE by using PAUP* (Swofford 2003) to estimate parameters for site rate variation and transition/transversion ratio.

RESULTS

Comparison of approximations of the marginal likelihood: In all but trivial situations we cannot calculate L_M or its log value, l_M, analytically. Using simulated data, we compared the two different methods for approximating L_M: the thermodynamically estimated $\hat{\ell}^{(\mathrm{TI}_i)}$ using coupled scaling classes TI_i and the harmonic mean HM estimated as $\hat{\ell}^{(\mathrm{HM})}$. In the context of coalescent simulations the artificial data D_i simulated from a set of true parameter values still include considerable variability, so we do not expect a particular $\hat{\ell}_M$ (for short: $\hat{\ell}$) from all data sets. Nevertheless, we expect that the different approximations will result in the same $\hat{\ell}$ for a specific data set. Figure 3 shows a comparison of the two different approximations of l_M. The relative magnitude of $\hat{\ell}$ among the different data sets is the same: a data set that shows low $\hat{\ell}$ with the HM estimator also shows low values for the different TI schemes. $\hat{\ell}^{(\mathrm{HM})}$ is little affected by the number of scaling classes, whereas the number of scaling classes affects the absolute value of the $\hat{\ell}^{(\mathrm{TI})}$. When the results of a specific data set are compared, the TI_4 method delivers lower $\hat{\ell}$ than the HM_4, HM_{16}, HM_{32}, TI_{16}, and TI_{32} methods. The thermodynamically estimated $\hat{\ell}^{(\mathrm{TI}_c)}$ using independent scaling classes is identical to the coupled scaling classes (data not shown).

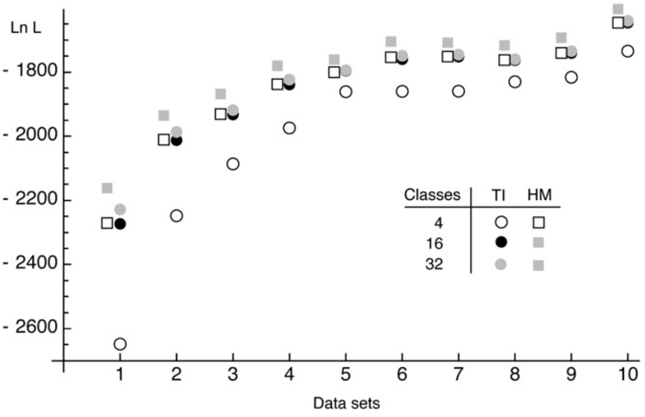

Figure 3.—Comparison of the log marginal likelihood l_M inferred by harmonic mean (HM) and thermodynamic integration (TI), using 4, 16, and 32 scaling classes of 10 independent data sets (sorted by magnitude of the likelihood of the TI runs with four scaling classes). HM values for the 16- and 32-chain runs were so similar that the squares overlap on the *y*-axis scaling used, but are different up to 5 log-likelihood units. The simulated data were generated using model $M =$ □←■.

Bayes factor estimation: Instead of reporting BF, we report its log-equivalent LBF, which is $\ln(L_{M_2}/L_{M_1})$ or $(\ell_{M_2} - \ell_{M_1})$. The log marginal-likelihood values $\hat{\ell}$ are dependent on the approximation, and the LBF depends on the difference of the log marginal likelihoods $\hat{\ell}$ and therefore the relative difference among models is more important than the unbiased recovery of $\hat{\ell}$ (Figure 3). Figure 4 compares the dependency of the approximations on the length of the run. The shortest run took only 5 sec with four chains, visiting 30,000 states and discarding the first 10,000; the longest four-chain run took 5 min 21 sec, visiting and discarding 256 times more states. The thermodynamic integration approximation results in LBFs with high repeatability and little variance even with only short runs, whereas the LBFs using the HM estimator are unstable even for long runs, and it appears that MCMCMC searches with many chains result in reduced reliability of the HM estimators.

Numerous artificial single-locus data sets from a model with two populations of unequal size, in which only one population receives migrants from the other, were generated; this model has three parameters that are free to vary: population sizes 1 and 2 and immigration rate from population 2 to population 1, which is $M_0 =$ □←■. Populations are indicated by squares. Two open squares indicate populations constrained to have the same size; one open and one solid square indicate population sizes are not constrained. Arrows indicate allowed migration direction [from population 1 to 2, from 2 to 1, or in both directions; arrows with two heads indicate symmetric migration rate parameters ($M = m/\mu$)]. These data sets were analyzed with all nine possible simple models (one parameter, □; two parameters, □↔■, □→■, □←□; three parameters, □→■, □←■, □↔■, □⇆□; four parameters, □⇆■); models that exclude gene flow among the populations were

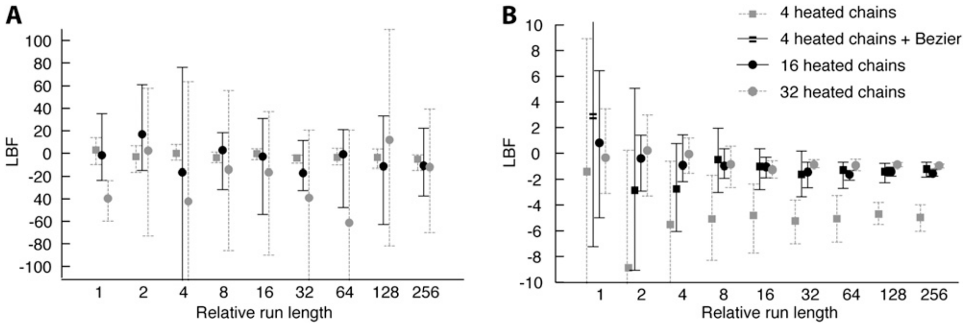

FIGURE 4.—Comparison of the LBF (ln BF) values for different run lengths of the MCMC chain. The squares and circles are LBF values using the average marginal likelihoods from five replicated runs. The vertical bars mark the range between the largest and the smallest LBF value from five replicated runs. (A) LBF approximated using the harmonic mean; (B) LBF approximated by thermodynamic integration. The simulated data were generated using model $M = \square\leftarrow\blacksquare$ and LBF $= (\ell_{\square\rightarrow\blacksquare} - \ell_{\square\leftarrow\blacksquare})$. LBF scales in A and B are very different.

omitted. We calculated log Bayes factors, LBF $= (\hat{\ell}_{M_i} - \hat{\ell}_{M_0})$. These report the chance of accepting M_i over M_0. In Table 2 LBF using TI_{16} rejects models that have more parameters than the true model or that disregard unidirectional migration with high frequency. Very simple models and asymmetric models are often accepted as plausible models. LBF using HM is indecisive, even with models that are very different from the true model, such as $\square\leftrightarrow\square$. Overall, the estimates from TI deliver a clearer guide about which models to prefer than the highly variable HM estimates (see File S1), which, on average, are less decisive.

A comparison with different strengths of migration rate among two populations (Table 3) shows that the $\mathrm{LBF}_{\mathrm{TI}_4}$ is more variable than the $\mathrm{LBF}_{\mathrm{TI}_{16}}$ but the numbers of acceptances or rejections of a hypothesis (Table 3, Table 2S in File S1) are very similar between TI_{16} and TI_4. In contrast, the $\mathrm{LBF}_{\mathrm{HM}}$ has a higher variability of outcomes.

Comparison with a panmixia test method: Currently, coalescence-based inference programs do not test whether the sampling locations are in separate populations or not. Therefore, summary statistics such as F_{ST}, Fisher's exact test, or population genetic clustering programs (PRITCHARD *et al.* 2000; EVANNO *et al.* 2005; HUELSENBECK and ANDOLFATTO 2007; MANEL *et al.* 2007; GUILLOT 2008) are being used to establish groups of individuals or sampling locations that most likely form panmictic populations. WAPLES and GAGGIOTTI (2006) showed that contingency table permutation methods work well. Hudson, Boos, and Kaplan (HUDSON *et al.* 1992a) developed a permutation test (HBK) that has great potential but seems to be little used despite its power to establish panmixia. For our comparison we used four scenarios: (1a) a single population was sampled and then the sample was randomly partitioned into two "populations", (1b) two populations exchanging 1250 migrants per generation, (2a) two populations exchanging 1 migrant every 4 generations, and (2b) two populations exchanging 1 migrant every 400 generations. Table 3 reveals that for a real panmictic population (1a), $\mathrm{LBF}_{\mathrm{TI}_{16}}$, $\mathrm{LBF}_{\mathrm{TI}_4}$, and $\mathrm{LBF}_{\mathrm{HM}}$ detect panmixia in 100, 94, and 73 of the data sets, respectively, whereas HBK finds that all 100 data sets are panmictic. Recognition of panmixia in scenario 1b was 100, 92, and 71 for $\mathrm{LBF}_{\mathrm{TI}_{16}}$, $\mathrm{LBF}_{\mathrm{TI}_4}$, and $\mathrm{LBF}_{\mathrm{HM}}$, respectively, whereas the HBK method marks all data sets panmictic. With $\mathrm{LBF}_{\mathrm{TI}}$, all data sets from scenario 2b fit a two-population model; with 2a the acceptance of a two-population model shrank to 70, 49, and 53 of 100, signaling considerable uncertainty about finding the correct population model. HBK declares all data sets under scenario 2 to contain

TABLE 2

Summary of support for specific models using LBF approximated with harmonic mean (HM) and thermodynamic integration (TI) using 16 chains with different scalers

Evidence ("true" $M_0 = \square\leftarrow\blacksquare$)	Counts (based on $\mathrm{LBF}_{\mathrm{TI}}$ and $\mathrm{LBF}_{\mathrm{HM}}$)															
n_{param}	4		3		3		3		2		2		2		1	
Model	□⇆■		□→■		□↔■		□⇆□		□←□		□→□		□↔□		□	
Approximation	TI	HM	TI	HM	TI	HM	TI	HM	TI	HM	TI	HM	TI	HM	TI	HM
Against M_0	0	46	28	36	0	48	0	57	70	50	54	35	0	59	11	40
Against M_i	100	54	72	64	100	52	100	43	30	50	46	65	100	41	89	60

One hundred single-locus data sets were analyzed, each with a total of 20 DNA sequences simulated using a three-parameter model with two different population sizes and unidirectional migration from population 2 to population 1 (model abbreviation is $\square\leftarrow\blacksquare$). All other models 1–8 (M_i), such as the full model (□⇆■) or the minimal model ($\square\leftrightarrow\square$), are compared with this "true" model ($\square\leftarrow\blacksquare$), which represents the M_0 hypothesis. n_{param}: number of parameter estimated.

TABLE 3

Comparison of the influence of the approximation on the power of LBF for simple models with different migration schemes

Evidence	Counts (based on $\mathrm{LBF}_{\mathrm{TI}_{16}}$, $\mathrm{LBF}_{\mathrm{TI}_4}$, and $\mathrm{LBF}_{\mathrm{HM}}$)											
Model		1a			1b			2a			2b	
Nm		∞			1250			0.25			0.0025	
Approximation	16	4	H	16	4	H	16	4	H	16	4	H
Against M_0	0	5	26	0	8	29	70	49	53	100	100	78
Against M_1	100	94	73	100	92	71	30	51	47	0	0	22

LBF compared a full model (model M_1 = □⇆■) with a panmictic population (model M_0 = □). Models used to simulate the data were as follows: 1a, a single population, the sampled individuals split randomly into two sets ($Nm \rightarrow \infty$); 1b, two populations exchanging many migrants ($Nm = 1250$); 2a, two populations exchanging a moderate number of migrants ($Nm = 0.25$); and 2b, two populations with very low migration rate ($Nm = 0.0025$). The marginal likelihoods used in the LBF were approximated with thermodynamic integration (TI) with 16 and 4 scaler bins and with the harmonic mean (HM_4).

two populations. $\mathrm{LBF}_{\mathrm{HM}}$ shows, for all scenarios, much larger variability in acceptance and rejection of panmixia (see File S1), resulting in a lower total acceptance of the correct model.

Effect of loci and model complexity: Table 4 shows the LBFs for six migration models (Table 1). The thermodynamic integration method consistently chooses the true model as the best model. Differences for the other models depend on the haphazard choice of the order of the loci. Because only 50 loci were simulated for all runs, the first locus is shared among all runs, and the second locus is shared among all runs except the 1-locus runs, etc. We expect that with many loci a clear order of models is achieved. The model order for the 50-locus run is 1, 2, 3, 6, 5, and 4. Runs with many loci (>10) suggest that the one-population model (5) is superior to the two-population model that combines the locations in an intermixed pattern (4) and also suggest that the 400-parameter (6) analysis is preferable over analyses with wrongly combined locations. Runs with only few loci may suffer because there are not enough data to correctly rank incorrect models 3, 4, 5, and 6. The reported Bayes factor values suggest that model 1 should be picked with probability 1.0 over the five alternatives. More loci increase this certainty considerably: the difference between the first and the second best model is already very large for a single locus. The number of loci and the BF differences are positively correlated. The results for the harmonic mean estimator suggest that the preferred model is the 9-parameter model (2) and not the model that was used to simulate the data (1).

TABLE 4

Comparison of log Bayes factors (marginal log-likelihood differences) approximated by thermodynamic integration and harmonic mean estimator, for different models and different numbers of loci

	LBF for model[a]						Rank of model					
	1	2	3	4	5	6	1st	2nd	3rd	4th	5th	6th
				Thermodynamic integration								
Loci												
1	0	−10	−86	−583	−594	−253	1	2	3	6	4	5
2	0	−552	−1,946	−3,167	−3,338	−467	1	6	2	3	4	5
5	0	−697	−2,432	−4,757	−4,826	−542	1	6	2	3	4	5
10	0	−1,136	−4,266	−8,566	−8,352	−2,328	1	2	6	3	5	4
20	0	−2,072	−5,914	−12,913	−12,379	−4,835	1	2	6	3	5	4
50	0	−4,829	−14,683	−30,147	−28,439	−15,245	1	2	3	6	5	4
				Harmonic mean estimator								
1	0	−7	−20	−29	−28	−35	1	2	3	5	4	6
2	0	−76	−83	−123	−70	−168	1	5	2	3	4	6
5	0	−124	−133	−215	−160	−308	1	2	3	5	4	6
10	0	−236	−201	−430	−161	−420	1	5	3	2	6	4
20	0	−438	−565	−1,085	−453	−943	1	2	5	3	6	4
50	0	−819	−1,266	−2,613	−1,266	−2,723	1	2	5	3	4	6

Model 1 was used to simulate the data and is the reference model.

[a] Model numbers are specified in Table 1.

TABLE 5

Log Bayes factors (LBF) estimated by thermodynamic integration and by the harmonic mean using different prior distributions

	Thermodynamic integration											
	LBF for model[a]						Rank of model					
Prior	1	2	3	4	5	6	1st	2nd	3rd	4th	5th	6th
Uniform narrow	0	−77	−108	−487	−540	−254	1	2	3	6	4	5
Uniform wide	0	−232	−165	−409	−277	−364	1	3	2	5	6	4
Exponential narrow	0	−17	−84	−531	−542	−255	1	2	3	6	4	5
Exponential wide	0	−170	−158	−461	−270	−394	1	3	2	5	6	4
	Harmonic mean estimator											
	LBF for model[a]						Rank of model					
Prior	1	2	3	4	5	6	1st	2nd	3rd	4th	5th	6th
Uniform narrow	0	−3	−29	−23	−4	−55	1	2	5	4	3	6
Uniform wide	0	−2	−18	−25	−25	−29	1	2	3	5[b]	4[b]	6
Exponential narrow	0	−8	−30	−23	−8	−37	1	5[b]	2[b]	4	3	6
Exponential wide	0	−8	−23	−36	−18	−55	1	2	5	3	4	6

Model 1 was used to simulate the data and is also the reference model.

[a] Model numbers are specified in Table 1.

[b] Tied.

Effects of prior distribution on the marginal likelihood: Table 5 reveals that the marginal likelihoods depend on the prior distribution: the LBF values are different for different prior distributions. For the thermodynamic integration method, however, the order of the models is identical among the narrow and wide prior distributions, respectively, suggesting that most likely the runs were rather short for the wide-prior models. The harmonic mean estimator of the marginal likelihood is similarly affected by the choice of prior distributions. Using the harmonic mean estimator, the models are ranked differently for each of the different priors.

Example analysis of migration patterns among humpback whales sampling locations in the south seas: Olavarría *et al.* (2007) and Engel *et al.* (2008) described the interaction of several humpback whale populations (sampling locations). We use parts of their data to showcase how BF can inform the discussion of whether whales from these sampling locations belong to the same genetic population or not and whether some population models provide more appropriate descriptions than others. Our analysis does not completely resolve the complex population interactions of humpback whales, but it shows ways in which our method is more useful than current methods for model comparisons. Engel *et al.* (2008), using pairwise F_{ST} estimates, suggested that Antarctic locations A1 and A2 appear panmictic; they used additional sighting data to suggest that the individuals sampled near the Brazilian coast probably do not move to the presumed feeding grounds in the Antarctic but instead aggregate at some unknown location. We chose a subset of models to investigate (1) whether the regions Antarctica 1 and 2 belong to a single population and (2) whether the Brazilian individuals and Antarctic individuals belong to the same population. Table 6 shows the $\hat{\ell}$ for each model tested for three subsets of the full data set. Model 6, which allows for structure between A1 and A2 and reduced gene flow between Antarctica and Brazil, has the highest marginal likelihood. This model was used as the reference in LBF to compare all models. Our analysis confirms the conclusion of Engel *et al.* (2008) that the connectivity between the Brazilian and Antarctic locations is reduced (model 6), but, unlike models 7–9, does not suggest complete isolation of the Brazilian individuals from the other locations. Model 2 is the second best model; it shares almost all features of model 6 except that the migration rates between Antarctica and Brazil are bidirectional. Models that suggest A1 and A2 are part of a panmictic population (models 3–5) have lower LBF values than models 2 and 6, but model 3 is superior to model 1. This suggests that A1 and A2 are probably not part of a panmictic population, but the data do not support a complex model with many parameters (model 1). Our current understanding of the population structuring is based on a single locus (mtDNA). These data are insufficient to resolve the complex interactions among southern Atlantic humpback whales.

The data sets were analyzed using TI with 32 chains and 4 chains. The Bézier-corrected 4-chain marginal likelihoods result in LBF of the same magnitude as the 32-chain runs, despite the greatly reduced run time.

DISCUSSION

The approximation of l_M using the harmonic mean estimator is concordant with the thermodynamic in-

TABLE 6

Log Bayes factor (LBF) using thermodynamic integration of different gene flow models M_i compared with model 6 for four sampling locations of humpback whales (C, Colombia; B, Brazil; A1, Antarctica east of the Antarctic peninsula; A2, Antarctica west of the Antarctic peninsula)

		LBF of nine models compared against M_6								
		1	2	3	4	5	6	7	8	9
Method	Samples	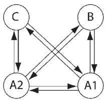	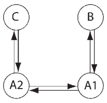	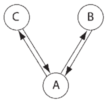	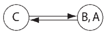	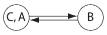	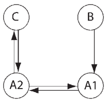	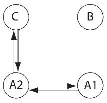	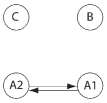	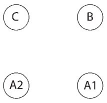
1	10[a]	−16.9	−6.1*		−21.2	−39.9	0.0***	−198.8	−241.7	−531.4
	10[a]	−17.0	−6.1*	−14.7	−39.3	−39.3	0.0***	−217.0	−194.1	−484.5
	10	−16.6	−4.5**	−13.8	−20.7	−36.8	0.0***	−237.3	−241.9	−523.8
	30	−91.3	−32.0	−84.4	−105.8	−227.9	0.0***	−291.4	−167.8	−605.5
2	10[a]	−15.1	−9.5	−13.9	−17.0	−29.0	0.0***	−180.0	−222.6	−494.3
	10[a]	−14.7	−9.3	−13.5	−16.3	−28.8	0.0***	−184.3	−193.8	−458.0
	10	−14.6	−7.8*	−12.4	−15.4	−25.2	0.0***	−276.2	−244.9	−501.8
	30	−75.0	−30.5	−77.0	−83.1	−164.6	0.0***	−189.4	−207.4	−663.2

Method 1, using 4 chains and Bézier approximation; method 2, using 32 chains. Model probabilities: *$0.01 < s_i < 0.05$; **$0.05 < s_i < 0.10$; and ***$0.9 < s_i < 1.0$.

[a] Same data, but different start values of the MCMC run.

tegration method, although the HM estimate is always higher than the TI estimator. Paul Lewis (P. Lewis, personal communication, 2009) has shown that this is an artifact of MCMC runs in which the HM estimator is biased toward the high probability regions of the parameter space. TI, in contrast, estimates very similar magnitudes of $\hat{\ell}$ over replicated runs of the same data and run parameters. Nevertheless, the magnitude of $\hat{\ell}$ using the thermodynamic method is correlated with the number of classes, although the relative difference among models persists independently of the absolute magnitude. Using the Bézier quadrature with a low number of chains at different scalers removes this difference. The run time is dependent on the number of chains, so the use of the Bézier quadrature may be preferable for large data sets and large population models because running many MCMC chains requires more time than is usually available in computer time budgets.

Analyses with different run lengths showed that the Bayes factor based on the harmonic mean estimator is more variable than that based on the thermodynamic integration estimator. Most disconcerting are the results with many chains because multiple LBF estimates based on the HM estimates show a wide range for the same data set, suggesting that an appropriate MCMC search results in unreliable HM estimates. The path of the MCMC chain influences the HM-based BF considerably because, for a good estimate of $\hat{\ell}$, the chain needs to explore areas of the solution space that have low probability. Once a low value is recorded, it affects the harmonic mean disproportionately. Runs that rarely visit such low values will report an $\hat{\ell}$ that is inflated. Using such values in the LBF_{HM} leads to high variance because the low values are not visited in the correct proportions. Our results corroborate the work of other authors (for example, Lartillot and Philippe 2006) who consider the HM inferior to the TI method.

The LBF usually supports the correct model independent of the number of chains used in the thermodynamic approximation method. In the comparison in Table 2, several models were weakly supported. This is interesting because these alternative models (□→■, □←□, □→□), which are models with strong unidirectional gene flow, are viable competitors for the real model (□←■) given the small sample size (20 individuals) and the large variance in coalescent simulations. Without multiple loci it is particularly difficult to estimate the migration direction from genetic data that often differ only in the frequency of alleles. The multilocus runs show the same general pattern as the analyses with few loci, but in the larger analyses the certainty of the order of models increases. The HM estimator is less certain for all scenarios than the TI estimator, corroborating the problems visible in Figure 4, suggesting again that the HM estimator should not be used.

LBF is relatively powerful for identifying appropriate models for samples from panmictic populations and well isolated populations, but showed a high variance for structured populations with moderate immigration rates (Table 3). In contrast, the Hudson–Boos–Kaplan estimator, using a permutation test, clearly suggested two populations for all analyzed data sets that were generated from models with reduced immigration rates. Because this test does not incorporate the uncertainty of the mutation model and the coalescence, however, it may overconfidently reject simpler (panmictic) interpretations.

It has been known for a while now through recent examples (Beerli and Felsenstein 1999; Felsenstein

2005; Heled and Drummond 2008) that the number of unlinked loci increases the accuracy of the coalescent estimators considerably; our comparison of the effect of multiple loci is no exception. Rejection of incorrect models became stronger with more loci when the marginal likelihood was approximated with thermodynamic integration. The harmonic mean estimator preferred a more complicated model with increased certainty, corroborating our findings with the two-population models (Tables 2 and 3) that the harmonic mean estimator should be avoided.

The Bayes factor framework demands proper priors, formally, priors that integrate to one. In our framework all priors are proper, although some may not be optimal: for example, uniform prior distributions over a very large range are wasteful because the posterior distribution covers only a small range of values and forces very long runs for accurate estimates. Our experimentation with different prior distributions shows that suboptimal priors can often result in long run times before convergence. The effect on the marginal likelihoods, however, seems small and the effect of such suboptimal priors on model choice seems negligible. In contrast, misspecification of the prior distribution, for example, choosing too narrow a prior distribution range, has a detrimental effect on the estimation of the posterior distribution of the parameters of the model and results in incorrect marginal likelihoods.

Our example (Table 6) confirms that, in a coalescence framework, a small sample per location has almost as much power as a large sample (*cf.* Felsenstein 2005) because not only is the LBF of a replicated run the same with the same sample, but also different randomly sampled sets of the same and larger size return the same ranking among the models. The Bézier-spline approximation of 4 chains gives LBF values that are equivalent to runs using 32 chains, but the run time is about one-eighth as long. This suggests that we are able to estimate LBF values of very large data sets in a reasonable time with good accuracy without the need to use a large number of chains or the reversible-jump MCMC (Green 1995) method that has recently been proposed by Lartillot (Lartillot and Philippe 2006) in a phylogenetic context. Our approach asks for independent runs for each model, in contrast to model selection approaches that use reversible-jump MCMC. This may look inelegant, but we believe that our method is preferable both because each run pays full attention to a single model and because the effort does not depend on the particular model-sampling algorithm and therefore is independent of the geometry of the complex solution space. In any study, the number of models depends on the number of populations and increases at a superexponential rate, so it is unlikely to evaluate all possible models, in contrast to mutation models, all of which are able to be evaluated (Huelsenbeck and Ronquist 2005). In addition, our scheme can be run in parallel without problems and without further programming.

The simulation study clearly shows that BFs are capable of distinguishing between different models and allow us to retrieve the model that was used to simulate the test data with high certainty when the true parameters produced a clear scenario. Single-locus data will often not be sufficient to retrieve a fairly complex model unambiguously, so that when available data are few, we should prefer simple models. Of course, multilocus data sets increase the certainty about the models considerably (Beerli and Felsenstein 1999; Heled and Drummond 2008).

We do not believe that our method should replace assignment- or allele-frequency-based methods, because for large problems the demand for large computer resources may make the analysis difficult or very time consuming. Our method does, however, add another tool for the researcher interested in natural population structures.

Our methods are available in the program MIGRATE from our website http://popgen.sc.fsu.edu. Simulated data sets and humpback whale example data sets are available at (http://people.sc.fsu.edu/~beerli/data) or upon request.

We thank Thomas Uzzell, Kathleen Lotterhos, and two anonymous reviewers for their critical comments of the text; Joseph Felsenstein and Anuj Srivastava for discussions, and Fred W. Huffer for checking our proofs for combining independently evaluated posterior distributions and marginal likelihoods. We also acknowledge the generous use of the High Performance Computing facility at Florida State University. This work was supported by the joint National Science Foundation (NSF)/National Institute of General Medical Sciences Mathematical Biology program under National Institutes of Health grant R01 GM 078985 and by NSF grant DEB 0822626.

LITERATURE CITED

Beerli, P., 1998 Estimation of migration rates and population sizes in geographically structured populations, pp. 39–53 in *Advances in Molecular Ecology* (NATO Science Series A: Life Sciences, Vol. 306), edited by G. Carvalho. IOS Press, Amsterdam,.

Beerli, P., 2004 Effect of unsampled populations on the estimation of population sizes and migration rates between sampled populations. Mol. Ecol. **13:** 827–836.

Beerli, P., 2006 Comparison of Bayesian and maximum likelihood inference of population genetic parameters. Bioinformatics **22:** 341–345.

Beerli, P., 2008 MIGRATE documentation (version 3.0). Technical Report. http://popgen.sc.fsu.edu.

Beerli, P., 2009 How to use MIGRATE or why are Markov chain Monte Carlo programs difficult to use? pp. 42–79 in *Population Genetics for Animal Conservation* (Conservation Biology, Vol. 17), edited by G. Bertorelle, M. W. Bruford, H. C. Hauffe, A. Rizzoli and C. Vernesi. Cambridge University Press, Cambridge, UK.

Beerli, P., and J. Felsenstein, 1999 Maximum-likelihood estimation of migration rates and effective population numbers in two populations using a coalescent approach. Genetics **152:** 763–773.

Beerli, P., and J. Felsenstein, 2001 Maximum likelihood estimation of a migration matrix and effective population sizes in *n* subpopulations by using a coalescent approach. Proc. Natl. Acad. Sci. USA **98:** 4563–4568.

Carstens, B., A. Bankhead, P. Joyce and J. Sullivan, 2005 Testing population genetic structure using parametric bootstrapping and MIGRATE-N. Genetica **124:** 71–75.

Corander, J., P. Marttinen, J. Sirén and J. Tang, 2008 Enhanced Bayesian modelling in BAPS software for learning genetic structures of populations. BMC Bioinformatics **9:** 539.

Engel, M. H., N. J. R. Fagundes, H. C. Rosenbaum, M. S. Leslie, P. H. Ott *et al.*, 2008 Mitochondrial DNA diversity of the Southwestern Atlantic humpback whale (Megaptera novaeangliae) breeding area off Brazil, and the potential connections to Antarctic feeding areas. Conserv. Genet. **9:** 1253–1262.

Evanno, G., S. Regnaut and J. Goudet, 2005 Detecting the number of clusters of individuals using the software STRUCTURE: a simulation study. Mol. Ecol. **14:** 2611–2620.

Felsenstein, J., 2005 Accuracy of coalescent likelihood estimates: Do we need more sites, more sequences, or more loci? Mol. Biol. Evol. **23:** 691–700.

Friel, N., and A. Pettitt, 2005 Marginal likelihood estimation via power posteriors. Technical Report 05-10, Department of Statistics, University of Glasgow, Glasgow, UK.

Friel, N., and A. Pettitt, 2008 Marginal likelihood estimation via power posteriors. J. R. Stat. Soc. Ser. B **70:** 589–607.

Gelman, A., and X.-L. Meng, 1998 Simulating normalizing constants: from importance sampling to bridge sampling to path sampling. Stat. Sci. **13:** 163–185.

Geyer, C. J., and E. A. Thompson, 1995 Annealing Markov-chain Monte-Carlo with applications to ancestral inference. J. Am. Stat. Assoc. **90:** 909–920.

Green, P. J., 1995 Reversible jump Markov chain Monte Carlo computation and Bayesian model determination. Biometrika **82:** 711–732.

Guillot, G., 2008 Inference of structure in subdivided populations at low levels of genetic differentiation—the correlated allele frequencies model revisited. Bioinformatics **24:** 2222–2228.

Heled, J., and A. J. Drummond, 2008 Bayesian inference of population size history from multiple loci. BMC Evol. Biol. **8:** 289.

Holsinger, K. E., P. O. Lewis and D. K. Dey, 2002 A Bayesian approach to inferring population structure from dominant markers. Mol. Ecol. **11:** 1157–1164.

Hudson, R. R., 1991 Gene genealogies and the coalescent process. Oxf. Surv. Evol. Biol. **7:** 1–44.

Hudson, R. R., D. D. Boos and N. L. Kaplan, 1992a A statistical test for detecting geographic subdivision. Mol. Biol. Evol. **9:** 138–151.

Hudson, R. R., M. Slatkin and W. P. Maddison, 1992b Estimation of levels of gene flow from DNA sequence data. Genetics **132:** 583–589.

Huelsenbeck, J., and P. Andolfatto, 2007 Inference of population structure under a Dirichlet process model. Genetics **175:** 1787–1802.

Huelsenbeck, J. P., and F. Ronquist, 2005 Bayesian analysis of molecular evolution using MrBayes, pp. 183–232 in *Statistical Methods in Molecular Evolution*, edited by R. Nielsen. Springer, New York.

Kass, R. E., and A. E. Raftery, 1995 Bayes factors. J. Am. Stat. Assoc. **90:** 773–795.

Kingman, J. F. C., 2000 Origins of the coalescent: 1974–1982. Genetics **156:** 1461–1463.

Kuhner, M., 2006 Lamarc 2.0: maximum likelihood and Bayesian estimation of population parameters. Bioinformatics **22:** 768–770.

Lartillot, N., and H. Philippe, 2006 Computing Bayes factors using thermodynamic integration. Syst. Biol. **55:** 195–207.

Manel, S., F. Berthoud, E. Bellemain, M. Gaudeul, J. E. Swenson *et al.*, 2007 A new individual-based geographic approach for identifying genetic discontinuities. Mol. Ecol. **16:** 2031–2043.

Michalakis, Y., and L. Excoffier, 1996 A generic estimation of population subdivision using distances between alleles with special reference for microsatellite loci. Genetics **142:** 1061–1064.

Neigel, J. E., 2002 Is F_{ST} obsolete? Conserv. Genet. **3:** 167–173.

Newton, M. A., and A. E. Raftery, 1994 Approximate Bayesian inference with the weighted likelihood bootstrap. J. R. Stat. Soc. Ser. B (Methodol.) **56:** 3–48.

Olavarría, C., C. Baker, C. Garrigue, M. Poole, N. Hauser *et al.*, 2007 Population structure of South Pacific humpback whales and the origin of the eastern Polynesian breeding grounds. Mar. Ecol. Prog. Ser. **330:** 257–268.

Palsbøll, P. J., M. Bérubé and F. Allendorf, 2007 Identification of management units using population genetic data. Trends Ecol. Evol. **22:** 11–16.

Pritchard, J. K., M. Stephens and P. Donnelly, 2000 Inference of population structure using multi-locus genotype data. Genetics **155:** 945–959.

Raymond, M., and F. Rousset, 1995 GENEPOP (version 1.2): population genetics software for exact tests and ecumenicism. J. Hered. **86:** 248–249.

Rousset, F., 1996 Equilibrium values of measures of population subdivision for stepwise mutation processes. Genetics **142:** 1357–1362.

Rousset, F., 2008 GENEPOP'007: a complete re-implementation of the GENEPOP software for Windows and Linux. Mol. Ecol. Res. **8:** 103–106.

Slatkin, M., 2005 Seeing ghosts: the effect of unsampled populations on migration rates estimated for sampled populations. Mol. Ecol. **14:** 67–73.

Strobeck, C., 1987 Average number of nucleotide differences in a sample from a single subpopulation: a test for population subdivision. Genetics **117:** 149–153.

Swofford, D. L., 2003 PAUP*. Phylogenetic Analysis Using Parsimony (*and Other Methods). Version 4. Sinauer Associates, Sunderland, Massachusetts.

Waples, R., and O. E. Gaggiotti, 2006 What is a population? An empirical evaluation of some genetic methods for identifying the number of gene pools and their degree of connectivity. Mol. Ecol. **15:** 1419–1439.

Weir, B. S., and W. G. Hill, 2002 Estimating F-statistics. Annu. Rev. Genet. **36:** 721–750.

Communicating editor: M. Stephens

APPENDIX

Independent calculation of marginal likelihoods: Maximum-likelihood inference for a multilocus data set can be run concurrently because, assuming the loci are independent, the calculation for each locus can be easily parallelized, and the final result is a simple combination of the individual results. In Bayesian inference, the independent calculation of the posterior distribution for each locus is simple. In contrast to the combination of maximum-likelihood estimates over loci, however, the product of these posterior distributions leads to an overuse of the prior. Correction for this overuse allows us to calculate the posterior distributions independently on different computers or CPU cores, therefore improving the speed of analysis considerably. The calculation of marginal likelihoods of a multilocus data set with independent calculations for each locus is difficult because the individual marginal likelihoods cannot be simply combined as in the maximum-likelihood analysis: there are interdependencies among the prior and the posterior distributions. Therefore, a scaling factor is needed for the combination of the locus-specific marginal likelihoods. Here we show how to correct for the overuse of priors and how to evaluate the multilocus marginal likelihoods that are generated from these independent posterior evaluations.

The combination of posteriors over multiple loci was done naively in our program MIGRATE (Beerli 2006); we overused the priors. This resulted in biases when the priors are highly skewed and do not match the posterior distribution. Analyses with uniform priors or single-locus analysis with any prior were not biased toward the prior mode.

Theorem 1. *The posterior*

$$P(\theta \mid D_1, D_2, \ldots, D_n) = \frac{P(\theta) \prod_i^n P(D_i \mid \theta)}{\int_\theta P(\theta) \prod_i^n P(D_i \mid \theta) d\theta} \qquad \text{(A1)}$$

with independent locus data $D_1, D_2, \ldots, D_n$, and a set of parameters θ can be calculated by

$$P(\theta \mid D_1, D_2, \ldots, D_n) = \frac{P(\theta)^{1-n} \prod_i^n P(\theta \mid D_i)}{\int_\theta P(\theta)^{1-n} \prod_i^n P(\theta \mid D_i) d\theta}. \qquad \text{(A2)}$$

Proof. Expanding $P(\theta \mid D_i)$ in (A2) leads to

$$P(\theta \mid D_1, D_2, \ldots, D_n) = \frac{P(\theta)^{1-n} \prod_i^n (P(\theta)P(D_i \mid \theta)/\int_\phi P(\phi)P(D_i \mid \phi)d\phi)}{\int_\theta P(\theta)^{1-n} \prod_i^n (P(\theta)P(D_i \mid \theta)/\int_\phi P(\phi)P(D_i \mid \phi)d\phi)d\theta}. \qquad \text{(A3)}$$

The integrals over ϕ cancel, so that

$$P(\theta \mid D_1, D_2, \ldots, D_n) = \frac{P(\theta)^{1-n} \prod_i^n P(\theta)P(D_i \mid \theta)}{\int_\theta P(\theta)^{1-n} \prod_i^n P(\theta)P(D_i \mid \theta)d\theta}. \qquad \text{(A4)}$$

Moving the $P(\theta)$ in (A4) out of the products results in equivalence of (A1) and (A2). ■

The denominator in (A2) can be built up during the MCMC run. The main difference between (A1) and (A2) is that the latter allows completely independent calculation for the unlinked loci and therefore allows easy distribution of the inference on a computer cluster or even computer grids, facilitating the analysis of data sets with many unlinked loci.

The Bayesian inference offers a convenient tool for comparing different population models without requiring that models be nested. The marginal likelihoods are normally not computed during an MCMC run because these normalizing weights cancel in comparisons during the run. They need to be computed and recorded, however, when the combined marginal likelihoods need to be calculated; to do that we must evaluate the denominator of (A1):

$$P(D_1, D_2, \ldots, D_n \mid M_i) = \int_\theta P(\theta \mid M_i) \prod_i^n P(D_i \mid \theta, M_i) d\theta. \qquad \text{(A5)}$$

Theorem 2. *The combined marginal likelihoods over all independent data blocks can be calculated as a product of independently calculated marginal likelihoods for each data block and a constant.*

Proof. The combined estimator of the posterior distribution is

$$P(\theta \mid D_1, \ldots, D_n, M_1) = \frac{P(\theta \mid M_1) \prod_i^n P(D_i \mid \theta, M_1)}{P(D_1, \ldots, D_n \mid M_1)}. \qquad \text{(A6)}$$

Converting the likelihoods using posteriors on the right,

$$\begin{aligned} P(\theta \mid D_1, \ldots, D_n, M_1) &= \frac{P(\theta \mid M_1) \prod_i^n P(\theta \mid D_i, M_1) P(D_i \mid M_1)}{P(\theta \mid M_1)^n P(D_1, \ldots, D_n \mid M_1)} \\ &= \frac{\prod_i^n P(\theta \mid D_i, M_1) P(D_i \mid M_1)}{P(\theta \mid M_1)^{n-1} P(D_1, \ldots, D_n \mid M_1)}, \end{aligned} \qquad \text{(A7)}$$

and moving $P(D_1, \ldots, D_n \mid M_1)$ to the left and $P(\theta \mid D_1, \ldots, D_n, M_1)$ to the right results in

$$P(D_1, \ldots, D_n \mid M_1) = \prod_i^n P(D_i \mid M_1) \frac{\prod_i^n P(\theta \mid D_i, M_1)}{P(\theta \mid M_1)^{n-1} P(\theta \mid D_1, \ldots, D_n, M_1)}. \qquad \text{(A8)}$$

The fraction has to be a constant with respect to θ because both the product of the individual marginal likelihoods and the combined marginal likelihood on the left are also constants with respect to θ:

$$K = \frac{\prod_i^n P(\theta \mid D_i, M_1)}{P(\theta \mid M_1)^{n-1} P(\theta \mid D_1, \ldots, D_n, M_1)}. \tag{A9}$$

Moving the combined posterior and integrating both sides with θ leads to a reexpression of *K*,

$$P(\theta \mid D_1, \ldots, D_n, M_1)K = \prod_i^n P(\theta \mid D_i, M_1) P(\theta \mid M_1)^{1-n} \tag{A10}$$

$$\int_\theta P(\theta \mid D_1, \ldots, D_n, M_1) K d\theta = \int_\theta \prod_i^n P(\theta \mid D_i, M_1) P(\theta \mid M_1)^{1-n} d\theta; \tag{A11}$$

and because

$$\int_\theta P(\theta \mid D_1, \ldots, D_n, M_1) d\theta = 1, \tag{A12}$$

$$K = \int_\theta \prod_i^n P(\theta \mid D_i, M_1) P(\theta \mid M_1)^{1-n} d\theta. \tag{A13}$$

This allows the calculation of the combined marginal likelihood using independent inferences

$$P(D_1, \ldots, D_n \mid M_1) = K \prod_i^n P(D_i \mid M_1). \tag{A14}$$

■

The denominator in (A2) is equivalent to *K* and has already been calculated during the MCMC run; it can be reused to calculate the combined marginal likelihoods.

Calculation of the scaling factor *K* in MIGRATE: In a Bayesian inference run of MIGRATE, *K* is calculated from the recorded posterior probabilities $P(\theta \mid D_i)$ and the prior $P(\theta)$ for a particular model *M* where θ are all the parameters of the model and D_i is the data for each unlinked locus. For example, in a simple one-parameter scenario, $\theta = \alpha$, we record α and its prior during the MCMC run. Then we construct a histogram of the α-values that represents the posterior distribution $P(\alpha \mid D)$. The prior distribution is also calculated at the values of the histogram columns. Summing over the histogram corrected for the overuse of the prior approximates the integral and calculates *K*. With a single locus, $K = 1$ and the "combined" marginal likelihood is the same as the single-locus marginal likelihood. With multiple parameters the integral will be multidimensional. If we assume that the parameters are independent of each other, the integration can be simplified. If we believe that the parameters are correlated, then we would need to calculate a multidimensional histogram; this is more tedious but certainly doable. MIGRATE uses the assumptions that parameters are independent because in our experience mutation-scaled migration rates and mutation-scaled population sizes are almost uncorrelated.

Specification of population models when some populations are isolated: MIGRATE uses two options to specify particular population models. The connection matrix allows the specification of directionality of gene flow, such as symmetric numbers of immigrants, symmetric immigration rates, average immigration rates, and immigration rates fixed to particular constants, for example, zero. If constants other than zero are used, then the start parameter settings need to be used in addition to the connection matrix to specify the values. This system allows approximating models where the populations are isolated from each other (Table 6) by inserting immigration rates that are very close to zero. For the humpback whale example we fixed all immigration rates to an isolated population as 100 times smaller than the mutation rate.

Run time considerations: The run time of MCMC programs is often difficult to predict because little automatic control can be given to users to check whether the MCMC chain has converged and enough samples from the desired distribution have been taken. Almost all applications have a tendency to sample too few steps along the MCMC chain. The faster a single step in the chain can be evaluated, the more steps can be sampled in the same time. The runs in this work all used similar run–parameter options (data sets and parameters are available in File S1). The run time values in Fig. 3 for data set 10 were 18 min using 4 different scaling classes, 70 min using 16 scalers, and 152 min using 32 scalers. In MIGRATE a deliberate decision was made not to farm out the Metropolis-coupled Markov chain sampling that is used for the thermodynamic integration; the run time increases proportionally with the number of chains. The expected run times based on the shortest run with 4 concurrent chains took 18 min (4 × 4.5 min), for 16 concurrent chains × 4.5 = 72 min, and for 32 × 4.5 = 144 min; the actual run times (18, 72, and 152 min) fit these values well. The run time is dependent on the number of sampling locations and the number of individuals in each location. For large data sets these values change to hours or days. Except for the 20-location example, we deliberately ran only small data sets for which we could easily establish convergence of the MCMC chain. Different Bayes factor runs are independent of each other and therefore one can run many models at the same time on a cluster. Many analyses in this work were run, in fact, on the high-performance cluster at Florida State University.

GENETICS

Supporting Information
http://www.genetics.org/cgi/content/full/genetics.109.112532/DC1

Unified Framework to Evaluate Panmixia and Migration Direction Among Multiple Sampling Locations

Peter Beerli and Michal Palczewski

DOI: 10.1534/genetics.109.112532

File S1

Unified Framework to Evaluate Panmixia and Migration Direction Among Multiple Sampling Locations Using Marginal Likelihoods

1 Comparison of simulated datasets: Expanded tables 2 and 3

Tables 2 and 3 in the article are abridged versions that do not highlight the strength of rejection of particular models. We present the full tables here and also give in Table 1S (Kass and Raftery 1995) the interpretation of the strength of support for the different values of the LBF. Table 2S and 3S give a more detailed answer than Table 2 and 3, but do not change the interpretation of the results. Unidirectional models models have high support even when the migration direction is incorrect when the number of parameters is small compared to the true model. Highest support among the incorrect models is given to the model with the correct migration direction and with constrained population sizes. It is worth noting that this support has a clear trend in the thermodynamic integration scheme; the harmonic mean estimator does not show such a trend, but shows a high variance.

Table 1S: Bayes factors and strength of acceptance of a model in comparison to a reference model (Kass and Raftery 1995). BF_{M_2,M_1} is the Bayes factor of model 2 versus model 1

$LBF_{M_2,M_1} = \log_e(\mathrm{BF}_{M_2,M_1})$	Evidence against Model 1
0 to 1	weak
1 to 3	positive
3 to 5	strong
>5	very strong

Table 2S: Comparison of the influence of the approximation on the power of LBF for simple models with different migration schemes. LBF compared a full model (Model $M_1 = \square \leftrightarrows \blacksquare$) with a panmictic population (Model $M_0 = \square$). Models used to simulate the data were: (1a) a single population ($Nm \to \infty$), the sampled individuals were split randomly into two sets; (1b) two populations exchanging many migrants ($Nm = 1250$); (2a) two population exchanging a moderate number of migrants ($Nm = 0.25$); and (2b) two populations with very low migration rate ($Nm = 0.0025$). The marginal likelihoods used in the LBF were approximated with thermodynamic integration (TI) with 16 and 4 temperature bins and with the harmonic mean (HM_4). The reported counts are the number of replicates that fall into the categories outlined in Table 1S

Evidence		Counts [based on $\mathrm{LBF}_{\mathrm{TI}_{16}}$,$\mathrm{LBF}_{\mathrm{TI}_4}$, LBF_{HM}]											
(M_0: one population)													
	Model		(1a)			(1b)			(2a)			(2b)	
	Nm		∞			1250			0.25			0.0025	
	Method	16	4	H	16	4	H	16	4	H	16	4	H
against M_0	very strong	0	1	0	0	2	0	32	34	0	100	100	59
	strong	0	1	1	0	2	0	10	6	1	0	0	3
	positive	0	0	5	0	0	5	18	5	18	0	0	11
	weak	0	3	20	0	4	24	10	4	34	0	0	5
	Total	0	5	26	0	8	29	70	49	53	100	100	78
against M_1	weak	1	1	40	4	1	38	13	4	33	0	0	5
	positive	6	3	31	4	3	30	10	3	13	0	0	2
	strong	35	8	5	32	8	3	7	7	1	0	0	0
	very strong	57	82	0	60	80	0	0	37	0	0	0	15
	Total	100	94	73	100	92	71	30	51	47	0	0	22

Table 3S: Summary of support for specific models using LBF approximated with harmonic mean (HM) and thermodynamic integration (TI) using 16 chains with different temperatures. 100 single-locus data sets were analyzed, each with a total of 20 DNA sequences simulated using a 3-parameter model with 2 different population sizes, and unidirectional migration from population 2 to 1 (Model abbreviation is $\square \leftarrow \blacksquare$; see Methods for details). All other models 1 to 8 (M_i), such as the full model ($\square \leftrightarrows \blacksquare$) or the minimal model ($\square$) are compared with this 'true' model ($\square \leftarrow \blacksquare$) that represent the M_0 hypothesis. n_{param} accounts for the number of parameter estimated.

Evidence																	
($M_0 = \square \leftarrow \blacksquare$)		Counts [based on $\mathrm{LBF}_{\mathrm{TI}}$ and $\mathrm{LBF}_{\mathrm{HM}}$]															
n_{param}		4		3		3		3		2		2		2		1	
Model		$\square \leftrightarrows \blacksquare$		$\square \rightarrow \blacksquare$		$\square \leftrightarrow \blacksquare$		$\square \leftrightarrows \square$		$\square \leftarrow \square$		$\square \rightarrow \square$		$\square \leftrightarrow \square$		$\square$	
Approximation		TI	HM	TI	HM	TI	HM	TI	HM	TI	HM	TI	HM	TI	HM	TI	HM
against M_0	very str.	0	1	0	0	0	3	0	4	0	1	0	1	0	1	9	10
	strong	0	4	1	2	0	1	0	1	0	4	0	3	0	6	0	1
	positive	0	22	3	13	0	23	0	27	20	21	17	17	0	28	0	16
	weak	0	19	24	21	0	21	0	25	50	24	37	14	0	24	2	13
		0	46	28	36	0	48	0	57	70	50	54	35	0	59	11	40
against M_i	weak	0	26	38	18	0	24	0	17	22	16	24	24	0	19	0	19
	positive	2	21	31	31	2	21	1	23	7	25	20	26	1	18	18	23
	strong	66	5	3	6	63	4	46	3	0	5	1	10	44	3	18	4
	very str.	32	2	0	9	35	3	53	0	1	4	1	5	55	1	53	14
		100	54	72	64	100	52	100	43	30	50	46	65	100	41	89	60
Different data sets		76	76	97	97	89	89	88	88	99	99	99	99	98	98	96	96

2 Run conditions for Figure 1

Ten artificial two-population data sets were created with the programs migtree and migdata using the following settings:

Mutation model	F84-model with transition/transversion ratio=2.0	
Mutation rate	2×10^{-6}	
Sequence length	1000	
Population model	Population 1	Population 2
Population size $N_e^{(i)}$	625	1250
Immigration rate m_{ji}	0.0002	0.0
Sample size	10	10

Each data set was run under 3 different heating schemes with the following temperature settings:

Chains	Temperature settings $T_i = 1/t_i$. Ordering is $T_1 ... T_n$
4	1.0, 1.5, 3.0, 1000000.0
16	1.0, 1.071, 1.154, 1.25, 1.364, 1.5, 1.667, 1.875, 2.143, 2.5, 3.0, 3.75, 5.0, 7.5, 15.0, 1000000.0
32	1.0, 1.03, 1.069, 1.107, 1.148, 1.19, 1.24, 1.29, 1.35, 1.41, 1.48, 1.55, 1.63, 1.72, 1.82, 1.94, 2.07, 2.21, 2.38, 2.58, 2.82, 3.10, 3.44, 3.875, 4.429, 5.167, 6.2, 7.75, 10.33, 15.5, 31.0, 1000000.0

All other settings were at the default values except the following:

Increment (sampling every x state)	1,000
Sampled states	20,000
Discarded states	1,000,000

3 Run conditions for Figure 3

One random dataset from the artificial data sets used in Figure 1 was used. Same temperatures as for Figure 1, but run parameters where changed to

Relative run-length	Increment (sampling every x state)	Sampled states	Discarded states
1	100	200	10,000
2	100	400	20,000
4	100	800	40,000
8	100	1,600	80,000
16	100	3,200	160,000
32	100	6,400	320,000
64	100	12,800	640,000
128	100	25,600	1,280,000
256	100	51,200	2,560,000

4 Run conditions for Figure 4

Run conditions were identical to figure 1.

5 Run conditions for Table 2

100 artificial data sets for the Model *xx0x* were generated:

Population model	Parameters	Population 1	Population 2
Two populations	Population size $N_e^{(i)}$	625	1250
(Model □ ← ■)	mutation rate	2×10^{-6}	
	Immigration rate m_{ji}	0.0002	0.0
	Sample size	10	10

The mutation model was F84 with a mutation rate of 0.000002. Each sequence was 1000 base pairs long. All run parameters were identical to Figure 1, but the runs used different population models as indicated in Table 2. The runs were executed on the High-performance cluster at Florida State University using the commonly available backfill queue. This queue allows runs maximally 4 hours long, which resulted in some table cells with fewer than 100 runs. A total of 900 runs were executed for Table 2.

6 Run conditions for Table 3

100 artificial data sets for each of the following population models were generated:

Population model	Parameters	Population 1	Population 2
Single population	Population size $N_e^{(i)}$	1250	-
(Model 1a)	Mutation rate	2×10^{-6}	
	Immigration rate m_{ji}	-	-
	Sample size	20	
Two populations	Population size $N_e^{(i)}$	625	625
(Model 1b)	Mutation rate	2×10^{-6}	2×10^{-6}
	Immigration rate m_{ji}	1.0	1.0
	Sample size	10	10
Two populations	Population size $N_e^{(i)}$	625	625
(Model 2a)	Mutation rate	2×10^{-6}	2×10^{-6}
	Immigration rate m_{ji}	0.0002	0.0002
	Sample size	10	10
Two populations	Population size $N_e^{(i)}$	625	625
(Model 2b)	Mutation rate	2×10^{-6}	2×10^{-6}
	Immigration rate m_{ji}	0.000002	0.000002
	Sample size	10	10

The mutation model was F84 with a mutation rate of 0.000002. Each sequence was 1000 base pairs long. All run parameters were identical to Figure 1. Each data set was run twice for each of the approximation methods (TI_4, TI_{16}), with the single population model *x* and with the unrestricted two-population model *xxxx*.

7 Run conditions for Table 4: Effect of number of loci on Bayes factors

All parameter settings were default, except

Prior distribution for mutation-scaled population size	Uniform with range 0.0 to 0.1
Prior distribution for mutation-scaled migration rates	Uniform with range 0.0 to 1000
Increment between samples	100
Samples per replicate	1,000
Burn-ins per replicate	100,000
Replicates	10
Heating	static with temperatures 1, 1.5, 3, 10^6

8 Run conditions for Table 5: Effect of prior distribution on Bayes factors

All parameter settings were default, except

Type	Priors for	
	Mutation-scaled population size	Mutation-scaled migration rates
	Minimum – Mean – Maximum	Minimum – Mean – Maximum
Uniform narrow	0 – 0.05 – 0.1	0.0 – 2500 – 5000
Uniform wide	0 – 0.25 –0.1	0.0 – 25,000 – 50,000
Exponential narrow	0 –0.01 – 0.1	0.0 – 100 – 5,000
Exponential wide	0 – 0.1– 0.5	0.0 – 2,000 – 50,000

9 Run conditions for Table 6: Humpback whale example

Mutation model	F84-model
Transition/transversion ratio	11.400000
Site rate modifier (3 groups)	0.416751 2.274676 6.216591
Probabilities of site rates	0.708460 0.280989 0.010551
Prior distribution for mutation-scaled population size	Uniform with range 0.0 to 0.1
Prior distribution for mutation-scaled migration rates	Uniform with range 0.0 to 5000
Increment between samples	200
Samples per replicate	5,000
Burn-ins per replicate	100,000
Replicates	50

Proposal distribution for parameters was Slice-sampling, whereas the genealogy proposals were using Metropolis-Hastings.